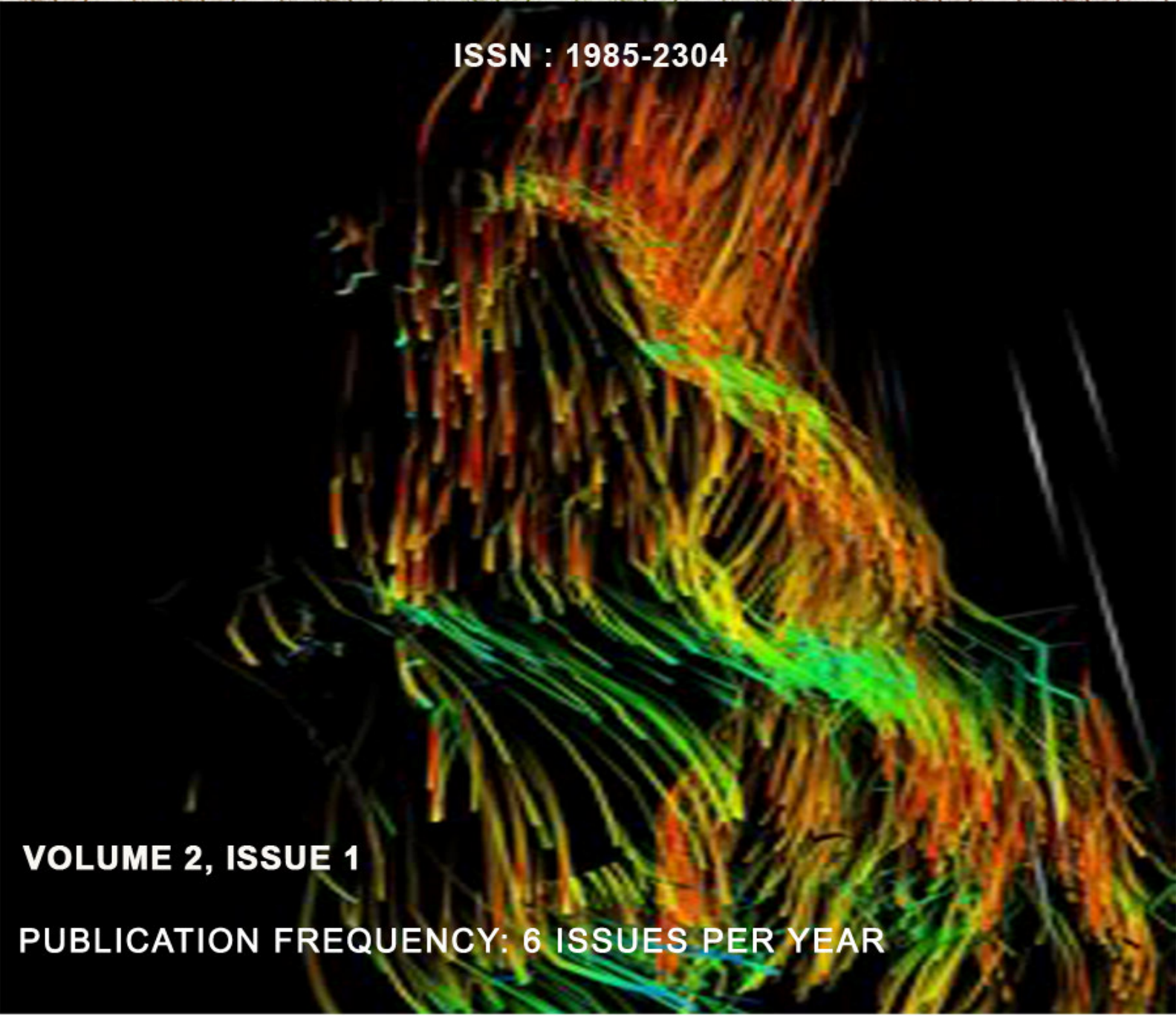


International Journal of Image Processing (IJIP)

ISSN : 1985-2304



VOLUME 2, ISSUE 1

PUBLICATION FREQUENCY: 6 ISSUES PER YEAR

Copyrights © 2008 Computer Science Journals. All rights reserved.

Editor in Chief Professor Hu, Yu-Chen

International Journal of Image Processing (IJIP)

Book: 2008 Volume 2, Issue 1

Publishing Date: 28-02 -2008

Proceedings

ISSN (Online): 1985-2304

This work is subjected to copyright. All rights are reserved whether the whole or part of the material is concerned, specifically the rights of translation, reprinting, re-use of illustrations, recitation, broadcasting, reproduction on microfilms or in any other way, and storage in data banks. Duplication of this publication or parts thereof is permitted only under the provision of the copyright law 1965, in its current version, and permission of use must always be obtained from CSC Publishers. Violations are liable to prosecution under the copyright law.

IJIP Journal is a part of CSC Publishers

<http://www.cscjournals.org>

©IJIP Journal

Published in Malaysia

Typesetting: Camera-ready by author, data conversion by CSC Publishing Services – CSC Journals, Malaysia

CSC Publishers

Table of Contents

Volume 2, Issue 1, February 2008.

Pages

- 1 – 9 fMRI Segmentation Using Echo State Neural Network
D.Suganthi, Dr.S.Purushothaman.
- 10 - 17 Content Based Image Retrieval using Color Boosted Salient
Points and Shape features of an image
Hiremath P.S, Jagadeesh Pujari.
- 18 – 26 Multi-Dimensional Features Reduction of Consistency Subset
Evaluator on Unsupervised Expectation Maximization Classifier for
Imaging Surveillance Application
Chue-Poh Tan, Ka-Sing Lim, Weng-Kin Lai.
- 27 - 34 Segmentation of Brain MR Images for Tumor Extraction by
Combining Kmeans Clustering and Perona-Malik Anisotropic
Diffusion Model
M. Masroor Ahmed, Dzulkifli Bin Mohammad

fMRI SEGMENTATION USING ECHO STATE NEURAL NETWORK

D.Suganthi

Research Scholar

Mother Teresa Women's University

Kodaikanal, Tamilnadu, INDIA

suganthi_d2@yahoo.com

Dr.S.Purushothaman

Principal

Sun College of Engineering & Technology

Kanyakumari – 629902, Tamil Nadu, INDIA

dr.s.purushothaman@gmail.com

Abstract

This research work proposes a new intelligent segmentation technique for functional Magnetic Resonance Imaging (fMRI). It has been implemented using an Echostate Neural Network (ESN). Segmentation is an important process that helps in identifying objects of the image. Existing segmentation methods are not able to exactly segment the complicated profile of the fMRI accurately. Segmentation of every pixel in the fMRI correctly helps in proper location of tumor. The presence of noise and artifacts poses a challenging problem in proper segmentation. The proposed ESN is an estimation method with energy minimization. The estimation property helps in better segmentation of the complicated profile of the fMRI. The performance of the new segmentation method is found to be better with higher peak signal to noise ratio (PSNR) of 61 when compared to the PSNR of the existing back-propagation algorithm (BPA) segmentation method which is 57.

Keywords: Echo state neural network, Intelligent segmentation, functional magnetic resonance imaging, Back-propagation algorithm, Feature Extraction, Peak signal to noise ratio

1. INTRODUCTION

Medical imaging plays a vital role in the field of bio-medical engineering. Some of the organs of the human body require non-invasive approach to understand the defects such as tumor, cancer in different parts of the body. Study and analysis of brain are done through the images acquired by various modalities like X-ray, Computer Tomography (CT), Positron Emission Tomography (PET), Ultrasound (US), Single Photon Emission Computed Tomography (SPECT) etc. The present day to day study of brain is much preferred through functional magnetic resonance imaging (fMRI). The acquired fMRI image need to be preprocessed, registered and segmented for understanding the defects in the brain by physician. Current tomographic technologies in medical imaging enable studies of brain function by measuring hemodynamic changes related to changes in neuronal activity. The signal changes observed in functional magnetic resonance imaging (fMRI) are mostly based on blood oxygenation level dependent (BOLD) contrast and are usually close to the noise level. Consequently, statistical methods and signal averaging are frequently used to distinguish signals from noise in the data. In most fMRI setup, images are acquired during alternating task (stimulus) and control (rest) conditions.

Automatic tissue segmentation approaches for 3D magnetic resonance images for brain have been developed under three broad algorithms, namely classification-based, region-based and contour-based approaches. Anatomical knowledge, used appropriately, boost the accuracy and robustness of the segmentation algorithm. MRI segmentation strive toward improving the accuracy, precision and computation speed of the segmentation algorithms [10].

Statistical methods are used for determining non-parametric thresholds for fMRI statistical maps by resampling fMRI data sets containing block shaped BOLD responses. The complex dependence structure of fMRI noise precludes parametric statistical methods for finding appropriate thresholds. The non-parametric thresholds are potentially more accurate than those found by parametric methods. Three different transforms have been proposed for the resampling: whitening, Fourier, and wavelet transforms. Resampling methods based on Fourier and wavelet transforms, which employ weak models of the temporal noise characteristic, may produce erroneous thresholds. In contrast, resampling based on a pre-whitening transform, which is driven by an explicit noise model, is robust to the presence of a BOLD response [9].

A commonly used method based on the maximum of the background mode of the histogram, is maximum likelihood (ML) estimation that is available for estimation of the variance of the noise in magnetic resonance (MR) images. This method is evaluated in terms of accuracy and precision using simulated MR data. It is shown that this method outperforms in terms of mean-squared-error [11].

A fully automated, parametric, unsupervised algorithm for tissue classification of noisy MRI images of the brain has been done. This algorithm is used to segment three-dimensional, T1-weighted, simulated and real MR images of the brain into different tissues, under varying noise conditions [12]. Parametric and non-parametric statistical methods are powerful tools in the analysis of fMRI data [7].

Probabilistic approaches to voxel based MR image segmentation identify partial volumetric estimations. Probability distributions for brain tissues is intended to model the response function of the measurement system [8]. Maximum Posterior Marginal (MPM) minimization and Markov Field [13] were used for contextual segmentation. Functional MRI segmentation using fuzzy clustering technique is proposed for objective determination of tumor volumes as required for treatment monitoring. A combination of knowledge based techniques and unsupervised clustering, segment MRI slices of the brain. Knowledge based technique is essential both in time and accuracy to expand single slice processing into a volume of slices [14].

A method for semiautomatic segmentation of brain structures such as thalamus from MRI images based on the concept of geometric surface flow has been done. The model evolves by incorporating both boundary and region information following the principle of variational analysis. The deformation will stop when an equilibrium state is achieved [15]. Energy minimization algorithm provides a high quality segmentation due to region homogeneity and compactness. The graph algorithm for multiscale segmentation of three dimensional medical data sets has been presented [4].

2. PROBLEM DEFINITION

The proposed method focuses on a new segmentation approach using energy minimizing echo state neural network. Due to the complicated profiles of the brain, the new method helps in segmenting the profiles by learning the different states of the profile of fMRI. Statistical features are calculated from the fMRI. These features are learnt by the training phase of the ESN. The learnt weights are further used for segmentation of the fMRI during the testing phase.

3. ECHO STATE NEURAL NETWORK (ESN)

Artificial neural networks are computing elements which are based on the structure and function of the biological neurons [2]. These networks have nodes or neurons which are described by difference or differential equations. The nodes are interconnected layer-wise or intra-connected among themselves. Each node in the successive layer receives the inner product of synaptic weights with the outputs of the nodes in the previous layer [1]. The inner product is called the activation value.

Dynamic computational models require the ability to store and access the time history of their inputs and outputs. The most common dynamic neural architecture is the time-delay neural network (TDNN) that couples delay lines with a nonlinear static architecture where all the parameters (weights) are adapted with the back propagation algorithm (BPA). Recurrent neural networks (RNNs) implement a different type of embedding that is largely unexplored. RNNs are perhaps the most biologically plausible of the artificial neural network (ANN) models. One of the main practical problems with RNNs is the difficulty to adapt the system weights. Various algorithms, such as back propagation through time and real-time recurrent learning, have been proposed to train RNNs. These algorithms suffer from computational complexity, resulting in slow training, complex performance surfaces, the possibility of instability, and the decay of gradients through the topology and time. The problem of decaying gradients has been addressed with special processing elements (PEs).

The echo state network, Figure 1, with a concept new topology has been found by [3]. ESNs possess a highly interconnected and recurrent topology of nonlinear PEs that constitutes a “reservoir of rich dynamics” and contain information about the history of input and output patterns. The outputs of this internal PEs (echo states) are fed to a memory less but adaptive readout network (generally linear) that produces the network output. The interesting property of ESN is that only the memory less readout is trained, whereas the recurrent topology has fixed connection weights. This reduces the complexity of RNN training to simple linear regression while preserving a recurrent topology, but obviously places important constraints in the overall architecture that have not yet been fully studied.

The echo state condition is defined in terms of the spectral radius (the largest among the absolute values of the eigenvalues of a matrix, denoted by $(\|W\|)$ of the reservoir’s weight matrix ($\|W\| < 1$)). This condition states that the dynamics of the ESN is uniquely controlled by the input, and the effect of the initial states vanishes. The current design of ESN parameters relies on the selection of spectral radius. There are many possible weight matrices with the same spectral radius, and unfortunately they do not all perform at the same level of mean square error (MSE) for functional approximation.

ESN is composed of two parts [5]: a fixed weight ($\|W\| < 1$) recurrent network and a linear readout. The recurrent network is a reservoir of highly interconnected dynamical components, states of which are called echo states. The memory less linear readout is trained to produce the output [6]. Consider the recurrent discrete-time neural network given in Figure 1 with M input units, N internal PEs, and L output units. The value of the input unit at time n is

$$u(n) = [u_1(n), u_2(n), \dots, u_M(n)]^T,$$

The internal units are $x(n) = [x_1(n), x_2(n), \dots, x_N(n)]^T$, and

output units are $y(n) = [y_1(n), y_2(n), \dots, y_L(n)]^T$.

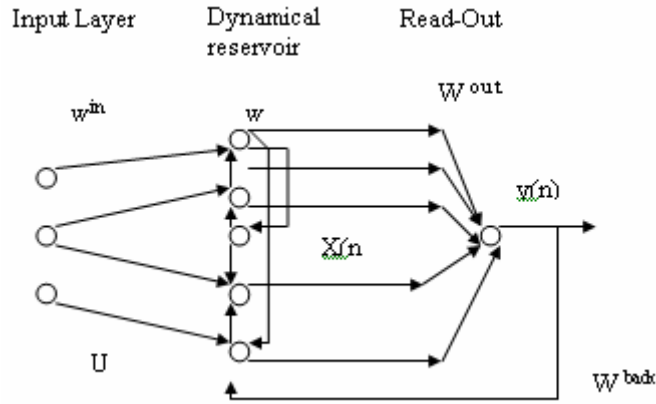


FIGURE 1: An echo state neural network

The connection weights are given

- in an $(N \times M)$ weight matrix $W^{back} = W_{ij}^{back}$ for connections between the input and the internal PEs,
- in an $N \times N$ matrix $W^{in} = W_{ij}^{in}$ for connections between the internal PEs
- in an $L \times N$ matrix $W^{out} = W_{ij}^{out}$ for connections from PEs to the output units and
- in an $N \times L$ matrix $W^{back} = W_{ij}^{back}$ for the connections that project back from the output to the internal PEs.

The activation of the internal PEs (echo state) is updated according to

$$x(n + 1) = f(W^{in} u(n + 1) + Wx(n) + W^{back}y(n)), \quad (1)$$

where

$f = (f_1, f_2, \dots, f_N)$ are the internal PEs' activation functions.

All f_i 's are hyperbolic tangent functions $\frac{e^x - e^{-x}}{e^x + e^{-x}}$. The output from the readout network is

computed according to

$$y(n + 1) = f^{out}(W^{out}x(n + 1)), \quad (2)$$

where

$f^{out} = (f_1^{out}, f_2^{out}, \dots, f_L^{out})$ are the output unit's nonlinear functions. The training and testing procedures are given in section 5.

4. PROPOSED METHOD FOR INTELLIGENT SEGMENTATION

In this work, much concentration is done for improving segmentation of fMRI by implementing the ESN. Figure 2 illustrates the sequence of steps involved in fMRI intelligent segmentation. Acquiring the image is done through standard fMRI equipment. The image is preprocessed to make sure that the noise is removed. Removal of noise is mostly preferred by using adaptive filtering methods. Depending on the severity of noise, the internal parameters of the filtering method can be fine tuned. Contrast enhancement of the image is done to have better clarity of the image.

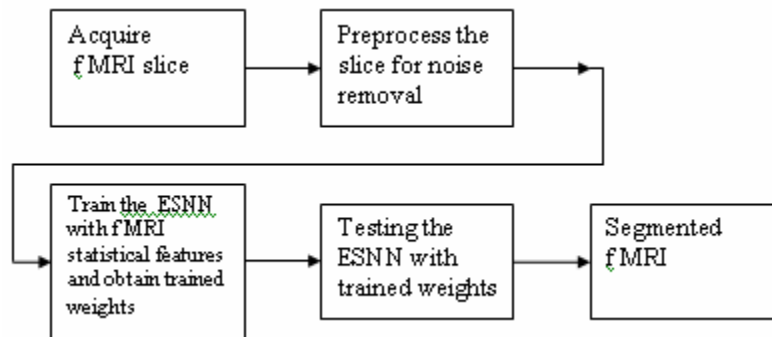


FIGURE 2: Schematic diagram of the Intelligent segmentation

This process is very important for further study of the fMRI slices. The ESN is initialized with random weights. The statistical features obtained from the FMRI are used to train the ESN. The process of training is used to obtain set of trained weights. Testing of ESN is done for fMRI segmentation using the trained weights.

5. IMPLEMENTATION OF SEGMENTATION USING ESN

Training of ESN to obtain trained weights

Step 1: Find the statistical features of the registered image

Step 2: Fix the target values(labeling)

Step 3: Set the no. of inputs, no. of reservoirs , no. of outputs

Step 4: Initialize weight matrices- no. of reservoirs versus no. of inputs, no.of outputs versus no. of reservoirs, no. of reservoirs versus no. of reservoirs

Step 5: Initialize temporary matrices.

Step 6: Find values of matrices less than a threshold

Step 7: Apply heuristics by finding eigenvector of updated weight matrices.

Step 8: Create network training dynamics and store the final weights.

Implementation of ESN for segmentation of fMRI using the trained weights of ESN

Step 1: Read the trained weights

Step 2: Input the statistical features of fMRI.

Step 3: Process the inputs and fMRI

Step 4: Apply transfer function

Step 5: Find the next state of the ESN.

Step 6: Apply threshold and segment the image

6. EXPERIMENTAL SETUP

The fMRI was obtained with standard setup conditions. The magnetic resonance imaging of a subject was performed with a 1.5-T Siemens Magnetom Vision system using a gradient-echo echoplanar (EPI) sequence (TE 76 ms, TR 2.4 s, flip angle 90°, field of view 256 - 256 mm, matrix size 64 * 64, 62 slices, slice thickness 3 mm, gap 1 mm), and a standard head coil. A checkerboard visual stimulus flashing at 8 Hz rate (task condition, 24 s) was alternated with a visual fixation marker on a gray background (control condition, 24 s).

7. RESULTS AND DISCUSSION

In Figure 3, some of the fMRI sequences have been displayed for clarity.

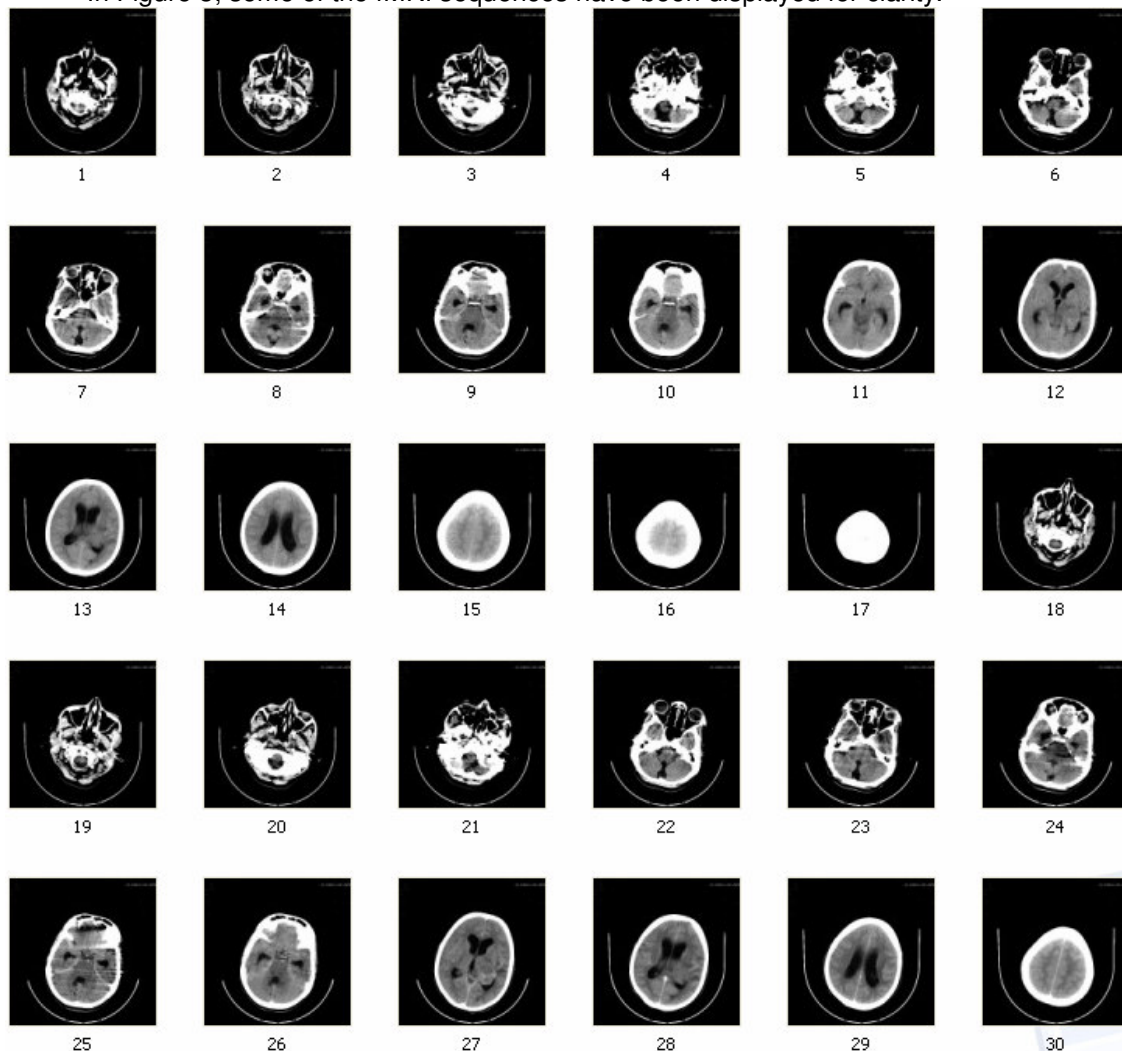
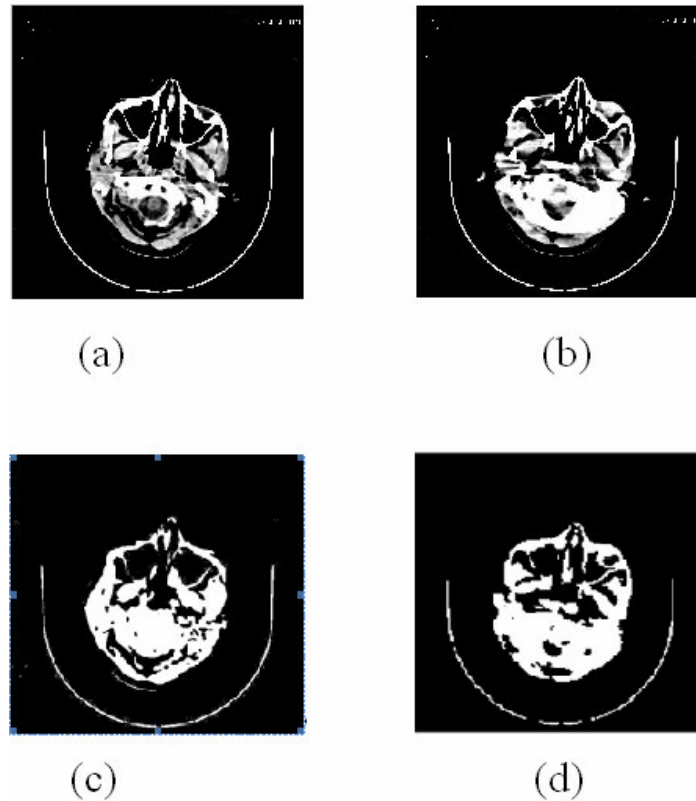


FIGURE 3: fMRI sequences

The image numbered (2) is considered for analyzing the performance of segmentation by ESN algorithm. As the initial image is affected with electronic noise, it has been adaptively filtered to remove the noise and subsequently registered.



- (a) Source-1
- (b) Source-1 filtered
- (c) BPA segmentation
- (d) ESN segmentation

FIGURE 4: Segmentation of fMRI –Sequence of outputs

For the comparison of the segmentation performances of the ESN, BPA segmentation is taken as the reference, since BPA is the oldest neural network method used earlier for image segmentation. The segmented image through BPA is shown in Figure 4(c). Similarly the segmented image using ESN is shown in Figure 4(d).

One of the important segmentation performance comparison is PSNR. The PSNR is expressed as

$$PSNR = 10 \cdot \log_{10} \left(\frac{255 \cdot 255}{MSE} \right) \dots \dots \dots (3)$$

$$MSE = \sum (\text{Original image} - \text{segmented image})^2$$

where

MSE is the mean squared error

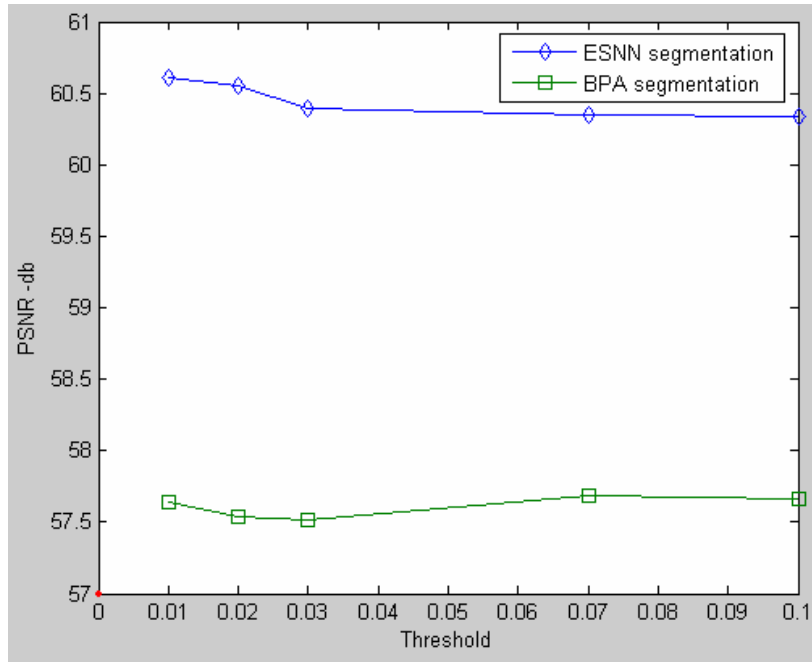


FIGURE 5: Comparison performance of ESN and BPA

Figure 5 shows peak signal to noise ratio for different threshold used in both the BPA and ESN algorithms. The PSNR values starts with minimum 57 and goes upto approximately 61. The range of PSNR for the segmented image using BPA is 57 to 58. The PSNR value for the segmented image by ESN ranges from 60 to 61. The maximum PSNR value is obtained in case of ESN segmentation is for threshold of 0.01 with 60.58. In case of segmentation by BPA, the maximum PSNR is only 57.9 for the threshold of 0.07. By comparison, the maximum PSNR is obtained at lower threshold for the ESN algorithm. The PSNR can be further improved by further modifying the ESN algorithm in terms of number of nodes I the hidden layer.

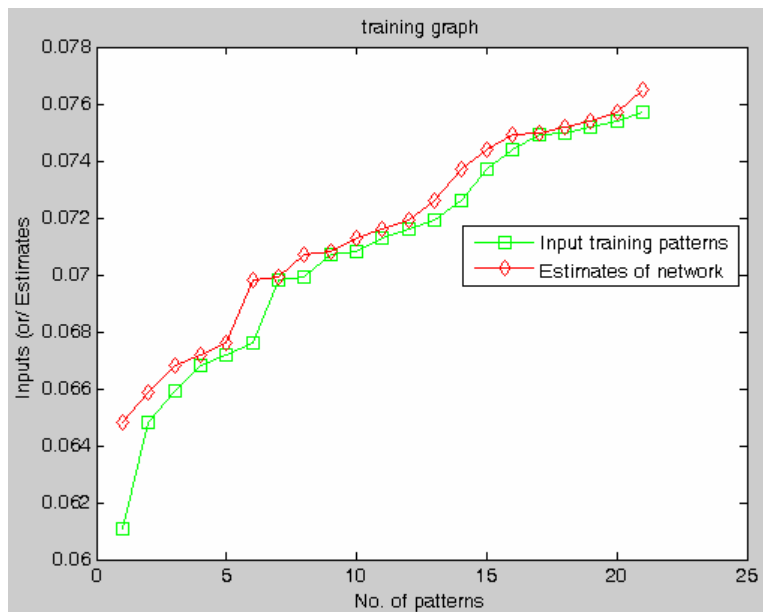


FIGURE 6: Training performance of the ESN

The Figure 6 shows the ESN estimation and the corresponding input patterns. The estimate is based on the number of reservoirs used during the training process.

8. CONCLUSION

The fMRI segmentation has been done with a recurrent ESN that stores the different states of fMRI. The PSNR value for this method is 60.6867. whereas, the PSNR value for the segmentation done by back-propagation algorithm is 55.67. The work can be further extended by incorporating modifications of internal states in ESN and fine tuning the noise filtering methods.

9. REFERENCES

- [1] Rumelhart D.E., Hinton G.E., and William R.J; Learning internal representations by error propagation, in Rumelhart, D.E., and McClelland, J.L.; Parallel distribution processing: Explorations in the microstructure of cognition; 1986.
- [2] Lippmann.R.P.; An Introduction to computing with neural nets, IEEE Transactions on ASSP Mag.,.35,4-22, 1987.
- [3] Jaeger, H.; The echo state approach to analyzing and training recurrent neural networks; (Tech. Rep. No. 148). Bremen: German National Research Center for Information Technology, 2001.
- [4] Brian Parker, Three-Dimensional Medical Image Segmentation Using a Graph-Theoretic Energy-Minimisation Approach ,Biomedical & Multimedia Information Technology (BMIT) Group, Copyright © 2002,
- [5] Jaeger, H;. *Short term memory in echo state networks*; (Tech. Rep. No. 152) Bremen: German National Research Center for Information Technology. 2002.
- [6] Jaeger, H.; *Tutorial on training recurrent neural networks, covering BPPT, RTRL,EKF and the "echo state network" approach* (Tech. Rep. No. 159).; Bremen: German National Research Center for Information Technology, 2002.
- [7] Sinisa Pajevica and Peter J. Basser, Parametric and non-parametric statistical analysis of DT-MRI data, Journal of Magnetic Resonance,1–14, 2003.
- [8] Thacker N. A., D. C. Williamson, M. Pokric; Voxel Based Analysis of Tissue Volume MRI Data;20th July 2003
- [9].Ola Friman and Carl-Fredrik Westin; Resampling fMRI time series; NeuroImage 25, 2005
- [10].Alan Wee-Chung Liew and Hong Yan; Current Methods in the Automatic Tissue Segmentation of 3D Magnetic Resonance Brain Images; *Current Medical Imaging Reviews*, 2006.
- [11] D. Poot, J. Sijbers,3A. J. den Dekker, R. Bos;Estimation of the noise variance from the background histogram mode of an mr image, *Proceedings of SPS-DARTS,2006*
- [12] Hayit Greenspan, Amit Ruf, and Jacob Goldberger, Constrained Gaussian Mixture Model Framework for Automatic Segmentation of MR Brain Images, IEEE Transactions On Medical Imaging, 25 (9), SEPTEMBER 2006
- [13] Abdelouahab Moussaoui, Nabila Ferahta, and Victor Chen; A New Hybrid RMN Image Segmentation Algorithm.; Transactions On Engineering, Computing And Technology, 12 ,2006
- [14]. Ruth Heller, Damian Stanley, Daniel Yekutieli, Nava Rubin, and Yoav Benjamini; Cluster-based analysis of FMRI data; NeuroImage 599–608, 2006
- [15] Greg Heckenberg, Yongjian Xi, Ye Duan, and Jing Hua; Brain Structure Segmentation from MRI by Geometric Surface Flow; International Journal of Biomedical Imaging ,1–6, 2006

Content Based Image Retrieval using Color Boosted Salient Points and Shape features of an image.

Hiremath P. S

*Department Of Computer Science,
Gulbarga University,
Gulbarga, Karnataka, India*

hiremathps@yahoo.co.in

Jagadeesh Pujari

*Department Of Computer Science,
Gulbarga University,
Gulbarga, Karnataka, India*

jaggudp@yahoo.com

Abstract

Salient points are locations in an image where there is a significant variation with respect to a chosen image feature. Since the set of salient points in an image capture important local characteristics of that image, they can form the basis of a good image representation for content-based image retrieval (CBIR). Salient features are generally determined from the local differential structure of images. They focus on the shape saliency of the local neighborhood. Most of these detectors are luminance based which have the disadvantage that the distinctiveness of the local color information is completely ignored in determining salient image features. To fully exploit the possibilities of salient point detection in color images, color distinctiveness should be taken into account in addition to shape distinctiveness. This paper presents a method for salient points determination based on color saliency. The color and texture information around these points of interest serve as the local descriptors of the image. In addition, the shape information is captured in terms of edge images computed using Gradient Vector Flow fields. Invariant moments are then used to record the shape features. The combination of the local color, texture and the global shape features provides a robust feature set for image retrieval. The experimental results demonstrate the efficacy of the method.

Keywords: *Color saliency, Local descriptors, Gradient vector flow field.*

1. INTRODUCTION

Content-based image retrieval (CBIR) [1,2,3,4] is a technique used for extracting similar images from an image database. The most challenging aspect of CBIR is to bridge the gap between low-level feature layout and high-level semantic concepts. In CBIR applications, the user typically provides an image (or a set of images) with no indication of which portion of the image is of interest. Thus a search in classical CBIR often relies upon a global view of the image. Localized CBIR [6] has been defined as a task where the user is only interested in a portion of the image and the rest is irrelevant.

To capture the local characteristics of an image, many CBIR systems either subdivide the image into fixed blocks [13,14], or more commonly partition the image into different meaningful regions by applying a segmentation algorithm [2,3,4]. In both the cases, each region of the image is represented as a feature vector of feature values extracted from the region. Other CBIR systems extract salient points (also known as interest points) [10,11,12], which are locations in an image where there is a significant variation with respect to a chosen image feature. With salient point methods, there is one feature vector created for each salient point. These representations enable a retrieval method to have a representation of different local regions of the image, and thus these images can be searched based on their local characteristics.

Usually the performance of a segmentation based method depends highly on the quality of the segmentation. Especially, a segmentation based representation usually measures features on a per-segment basis, and the average features of all pixels in a segment are often used as the features of that segment [3,4]. Therefore, this representation requires high quality segmentations because small areas of incorrect segmentation might make the representation very different from that of the real object. Moreover, the incorrect segmentation also hampers the shape analysis process. The object shape has to be handled in an integral way in order to be close to human perception. Shape has been extensively used for retrieval systems [8,9].

The salient point methods for retrieval assign features to a salient point based on the image features of all the pixels in a window around the salient point. Traditionally salient point detectors for CBIR often use the luminance component of the image for salient point computation, and thus, ignore the color information. The disadvantage of this method is that the salient points often gather at textured portions of the image or on the edges where the change of intensity is significant, so that many salient points capture the same portion of the image. This motivated us to develop a technique for image retrieval that uses color distinctiveness in determining the salient points and also that uses shape features in terms of the object edges. Different sized windows are used to capture the texture and color information around the salient points. Gradient Vector Flow (GVF) fields [7] are used to compute the edge image, which will capture the object shape information. GVF fields give excellent results in determining the object boundaries irrespective of the concavities involved. Invariant moments are used to serve as shape features. The combination of these features forms a robust feature set in retrieving applications. The experimental results are compared with those in [3,4].

The section 2 outlines the system overview and proposed method. The section 3 deals with experimental setup. The section 4 presents results. The section 5 presents conclusions.

2. SYSTEM OVERVIEW AND PROPOSED METHOD

The schematic block diagram of the proposed system based on color salient points is shown in Fig 1.

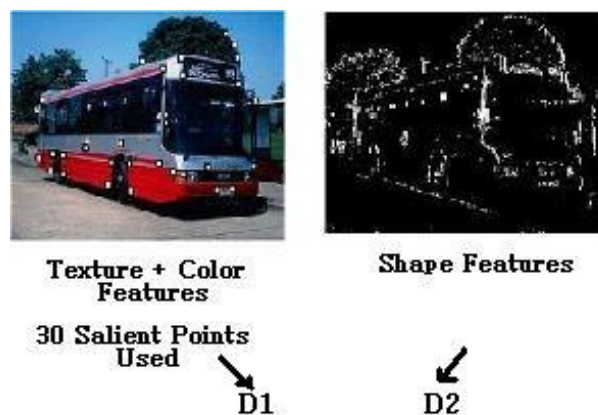


FIGURE 1: Overview of the proposed system.

2.1 COLOR DISTINCTIVENESS

The efficiency of salient point detection depends on the distinctiveness of the extracted salient points. At the salient points' positions, local neighborhoods are extracted and described by local image descriptors. The distinctiveness of the descriptor defines the conciseness of the representation and the discriminative power of the salient points. The distinctiveness of points of interest is measured by its information content. Most salient point detectors focus on two dimensional structures, such as corners, which are stable and distinctive at the same time. Color is also considered to play an important role in attributing image saliency. In our approach, the color saliency is based on the work reported in [16]. To achieve the color saliency, the color axes are rotated followed by a rescaling of the axis and, the oriented ellipsoids are transformed into spheres. Thus, the vectors of equal saliency are transformed into vectors of equal length. Fig. 2 shows the salient points detected using the Harris corner detector [12] and the proposed method. The salient points are circled in yellow and blue for Harris detector and the proposed method, respectively. The Harris detector detects points based on black and white events, while the proposed method uses color saliency to detect the events. It can be seen from the figure that the Harris detector detects salient points that typically cluster around textured areas, while the proposed method spreads them according to color saliency. In our experiments we have considered 30 salient points. The texture features were captured in a window of size 9 x 9 around every salient point and the color features in a window of size 3 x 3 around each salient point. The Fig. 3 illustrates this process. The procedure for computation of features is discussed in section 3.

2.2 SHAPE

Shape information is captured in terms of the edge image of the gray scale equivalent of every image in the database. We have used gradient vector flow (GVF) fields to obtain the edge image [7].

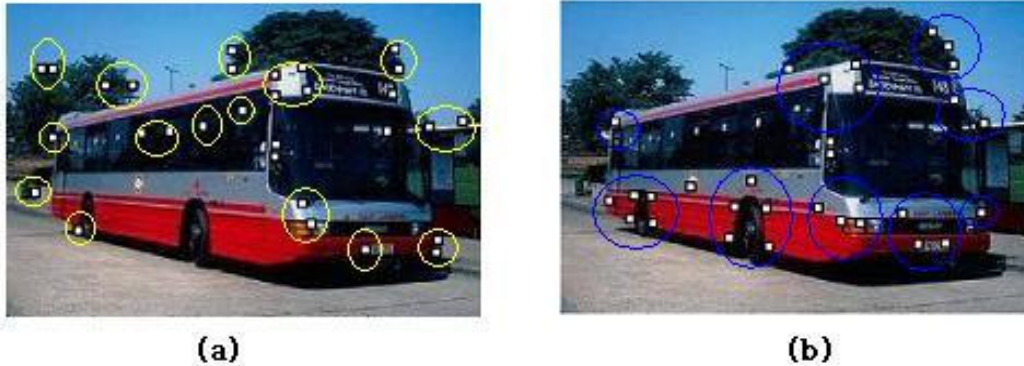


FIGURE 2: (a) Harris Corner Detector. (b) Proposed Method.

2.2.1 GRADIENT VECTOR FLOW:

Snakes, or active contours, are used extensively in computer vision and image processing applications, particularly to locate object boundaries. Problems associated with their poor convergence to boundary concavities, however, have limited their utility. Gradient vector flow (GVF) is a static external force extensively used in active contour method. GVF is computed as a diffusion of the gradient vectors of a grey-level or binary edge map derived from the images. The GVF uses a force balance condition given by

$$F_{int} + F_{ext}^{(p)} = 0$$

, where F_{int} is the internal force and $F_{ext}^{(p)}$ is the external force.

The external force field $F_{ext}^{(p)} = V(x, y)$ is referred to as the GVF field. The GVF field $V(x, y)$ is a vector field given by $V(x, y) = [u(x, y), v(x, y)]$ that minimizes the energy functional

$$\mathcal{E} = \iint \mu(u_x^2 + u_y^2 + v_x^2 + v_y^2) + |\nabla f|^2 |V - \nabla f|^2 dx dy$$

This variational formulation follows a standard principle, that of making the results smooth when there is no data. In particular, when $|\nabla f|$ is small, the energy is dominated by the sum of squares of the partial derivatives of the vector field, yielding a slowly varying field. On the other hand, when $|\nabla f|$ is large, the second term dominates the integrand, and is minimized by setting $V = |\nabla f|$. This produces the desired effect of keeping V nearly equal to the gradient of the edge map when it is large, but forcing the field to be slowly-varying in homogeneous regions. The parameter μ is a regularization parameter governing the tradeoff between the first term and the second term in the integrand.

The algorithm for edge image computation is given below:
Algorithm: (edge image computation)

1. Read the image and convert it to gray scale.
2. Blur the grey scale image using a Gaussian filter.
3. Compute the gradient map of the blurred image.
4. Compute GVF. (100 iterations and $\mu = 0.2$)
5. Filter out only strong edge responses using $k\sigma$, where σ is the standard deviation of the GVF. (k – value used is 2.5)
6. Converge onto edge pixels satisfying the force balance condition yielding edge image.

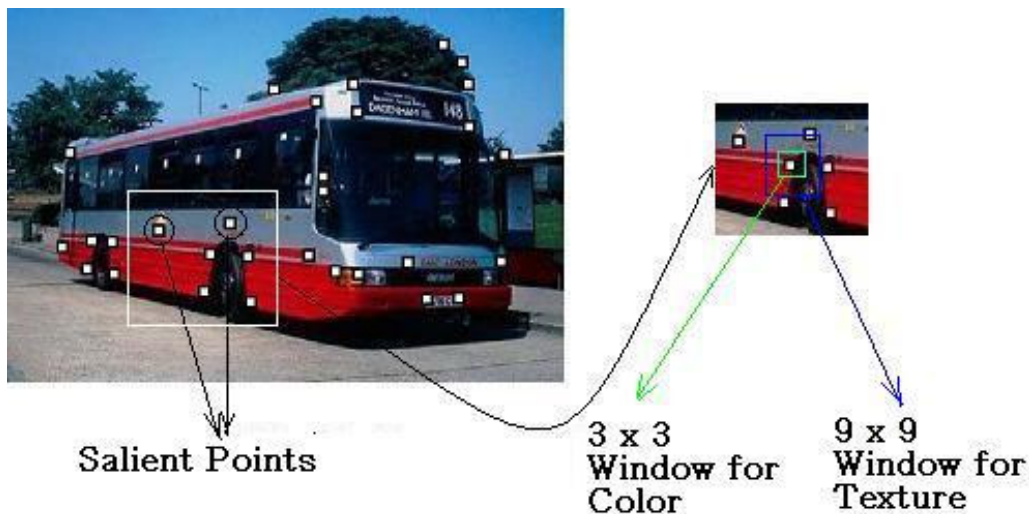


FIGURE 3: Feature Computation Process

3. EXPERIMENTAL SETUP

(a) Data set: Wang's [5] dataset consists of 1000 Corel images with ground truth. The image set comprises 100 images in each of 10 categories.

(b) Feature set: Texture and color features are explained below.

Texture: Gabor filter responses are used as texture features. 6 orientations and 4 scales are considered for this purpose [17]. A window of size 9 x 9 around every salient point is considered to capture the local texture features. First and second order statistical moments of the 24 filter responses, on the L component of the CIE-Lab space for the image, serve as the texture features. The responses were normalized over the entire image database.

Color: The first and second order statistical moments of the color bands, a and b, in the CIE-Lab color space of the image, are computed around every salient point within a window of size 3 x 3, as color features.

A total of 52 features are computed for each salient point. A total of 30 salient points are considered. Going beyond 30 salient points, did not yield considerable improvement in retrieval result worth the computational overheads involved.

The overall similarity distance D_j for the j^{th} image in the database is obtained by linearly combining the similarity distance of each individual feature:

$$d_j = \sum w_i s_j(f_i)$$

, with $S_j(f_i) = (x_i - q_i)^T(x_i - q_i)$, $j = 1, \dots, N$ and $i = 1, \dots, M$, where N is the total number of images in the database and M the total number of color and texture features. The low level feature weights w_i for color and texture are set to be equal.

Shape: Translation, rotation, and scale invariant one-dimensional normalized contour sequence moments are computed on the edge image [15]. The gray level edge images of the R, G and B individual planes are taken and the shape descriptors are computed as follows:

$$F_1 = \frac{(\mu_2)^{1/2}}{m_1}, \quad F_2 = \frac{\mu_3}{(\mu_2)^{3/2}}, \quad F_3 = \frac{\mu_4}{(\mu_2)^2}, \quad F_4 = \frac{\mu_5}{\mu_2}$$

where

$$m_r = \frac{1}{N} \sum_{i=1}^N [z(i)]^r, \quad \mu_r = \frac{1}{N} \sum_{i=1}^N [z(i) - m_1]^r, \quad \overline{\mu_r} = \frac{\mu_r}{(\mu_2)^{r/2}}$$

and $z(i)$ is set of Euclidian distances between centroid and all N boundary pixels.

A total of 12 features result from the above computations. In addition, moment invariant to translation, rotation and scale is computed on R, G and B planes individually considering all the pixels [15]. The transformations are summarized as below:

$$\eta_{pq} = \frac{\mu_{pq}}{\mu_{00}^\gamma}, \quad \text{where } \gamma = \frac{p+q}{2} + 1 \quad (\text{Central moments}) \quad \phi = \eta_{20} + \eta_{02}, \quad (\text{Moment invariant})$$

The above computations will yield an additional 3 features amounting to a total of 15 features.

Canberra distance measure is used for similarity comparison in all the cases. It allows the feature set to be in unnormalized form and is given by:

$$CanbDist(x, y) = \sum_{i=1}^d \frac{|x_i - y_i|}{|x_i| + |y_i|}$$

, where x and y are the feature vectors of database and query image, respectively, of dimension d . The distance between two images is computed as $D = D_1 + D_2$ where D_1 is the distance computed using color and texture information around the salient points and D_2 is the distance resulting from shape comparison..

4. EXPERIMENTAL RESULT

The experiments were carried out as explained in the sections 2 and 3.

The results are benchmarked with standard systems namely, SIMPLcity and FIRM, using the same database as in [3,4]. The quantitative measure defined is average precision as explained below:

$$p(i) = \frac{1}{100} \sum_{1 \leq j \leq 1000, r(i,j) \leq 100, ID(j)=ID(i)} 1$$

where $p(i)$ is precision of query image i , $ID(i)$ and $ID(j)$ are category ID of image i and j respectively, which are in the range of 1 to 10. The $r(i,j)$ is the rank of image j (i.e. position of image j in the retrieved images for query image i , an integer between 1 and 1000).

This value is the percentile of images belonging to the category of image i in the first 100 retrieved images.

The average precision p_t for category t ($1 \leq t \leq 10$) is given by

$$p_t = \frac{1}{100} \sum_{1 \leq i \leq 1000, ID(i)=t} p(i)$$

The results are tabulated in Table 1. The results of retrieval obtained using the Harris corner detector are also provided for the sake of comparison. In most of the categories our proposed method has performed at par or better than other systems. The results are considerably improved by considering color saliency in salient point detection as compared to grey scale salient points detected by Harris corner detector.

6. CONCLUSION

We have proposed a novel method for image retrieval using color, texture and shape features. Salient points based on color saliency are computed on the images. Texture and color features are extracted from fixed sized windows around these salient points to serve as local descriptors. Gradient vector flow fields are used to extract edge images of objects. Invariant moments are used to describe the shape features. A combination of these local color, texture and global shape features provides a robust set of features for image retrieval. The experiments using the Corel dataset demonstrate the efficacy of this method.

Class	SIMPLicity [4]	FIRM [3]	Proposed Method	
			With salient points detected by Harris Corner Detector	With color salient points
Africa	.48	.47	.40	.48
Beaches	.32	.35	.31	.34
Building	.35	.35	.32	.33
Bus	.36	.60	.44	.52
Dinosaur	.95	.95	.92	.95
Elephant	.38	.25	.28	.40
Flower	.42	.65	.58	.60
Horses	.72	.65	.68	.70
Mountain	.35	.30	.32	.36
Food	.38	.48	.44	.46

TABLE 1: Comparison of average precision obtained by proposed method with other standard retrieval systems SIMPLicity and FIRM.

6. REFERENCES

- [1] Ritendra Datta, Dhiraj Joshi, Jia Li and James Wang, "Image Retrieval: Ideas, Influences, and Trends of the New Age", Proceedings of the 7th ACM SIGMM international workshop on Multimedia information retrieval, November 10-11, 2005, Hilton, Singapore.
- [2] C. Carson, S. Belongie, H. Greenspan, and J. Malik, "Blobworld: Image Segmentation Using Expectation-Maximization & Its Application to Image Querying," in IEEE Trans. On PAMI, vol. 24, No.8, pp. 1026-1038, 2002.
- [3] Y. Chen and J. Z. Wang, "A Region-Based Fuzzy Feature Matching Approach to Content-Based Image Retrieval," in IEEE Trans. On PAMI, vol. 24, No.9, pp. 1252-1267, 2002.
- [4] . J. Li, J.Z. Wang, and G. Wiederhold, "IRM: Integrated Region Matching for Image Retrieval," in Proc. of the 8th ACM Int. Conf. on Multimedia, pp. 147-156, Oct. 2000.
- [5] <http://wang.ist.psu.edu>
- [6] R. Rahamani, S. Goldman, H. Zhang, J. Krettek and J. Fritts, "Localized content-based image retrieval", ACM workshop on Multimedia Image Retrieval, pp. 227-236, 2005.
- [7] Chenyang Xu, Jerry L Prince, "Snakes, Shapes, and Gradient Vector Flow", IEEE Transactions on Image Processing, Vol-7, No 3, PP 359-369, March 1998.
- [8] T. Gevers and A.W.M. Smeuiders., "Combining color and shape invariant features for image retrieval", Image and Vision computing, vol.17(7),pp. 475-488 , 1999.
- [9] A.K.Jain and Vailalya., "Image retrieval using color and shape", pattern recognition, vol. 29, pp. 1233-1244, 1996.
- [10] D.Lowe, "Distinctive image features from scale invariant keypoints", International Journal of Computer vision, vol. 2(6),pp.91-110,2004.

- [11] K. Mikolajczyk and C. Schmid, "Scale and affine invariant interest point detectors", *International Journal of Computer Vision*, vol. 1(60), pp. 63-86, 2004.
- [12] C. Harris and M. Stephens, "A combined corner and edge detectors", 4th Alvey Vision Conference, pp. 147-151, 1988.
- [13] Q. Tian, Y. Wu and T. Huang, "Combine user defined region-of-interest and spatial layout for image retrieval", *ICIP 2000*.
- [14] P. Howarth and S. Ruger, "Robust texture features for still-image retrieval", *IEE. Proceedings of Visual Image Signal Processing*, Vol. 152, No. 6, December 2005.
- [15] Dengsheng Zhang, Guojun Lu, "Review of shape representation and description techniques", *Pattern Recognition* Vol. 37, pp 1-19, 2004.
- [16] J. van de Weijer, Th. Gevers, J-M Geusebroek, "Boosting Color Saliency in Image Feature Detection", *IEEE Trans. Pattern Analysis and Machine Intelligence*, vol. 27 (4), April 2005.
- [17] B.S. Manjunath and W.Y. Ma, "Texture Features for Browsing and Retrieval of Image Data", *IEEE transactions on PAAMI*, Vol 18, No. 8, August 1996

Multi-Dimensional Features Reduction of Consistency Subset Evaluator on Unsupervised Expectation Maximization Classifier for Imaging Surveillance Application

Chue-Poh TAN

*Centre for Advanced Informatics
MIMOS Berhad
Technology Park Malaysia
57000 Kuala Lumpur, Malaysia.*

chue.poh@mimos.my

Ka-Sing LIM

*Faculty of Engineering,
Multimedia University,
Persiaran Multimedia,
63100 Cyberjaya, Selangor, Malaysia.*

kslim@mmu.edu.my

Weng-Kin LAI (Dr.)

*Centre for Advanced Informatics
MIMOS Berhad
Technology Park Malaysia
57000 Kuala Lumpur, Malaysia.*

weng.kin@mimos.my

Abstract

This paper presents the application of multi dimensional feature reduction of Consistency Subset Evaluator (CSE) and Principal Component Analysis (PCA) and Unsupervised Expectation Maximization (UEM) classifier for imaging surveillance system. Recently, research in image processing has raised much interest in the security surveillance systems community. Weapon detection is one of the greatest challenges facing by the community recently. In order to overcome this issue, application of the UEM classifier is performed to focus on the need of detecting dangerous weapons. However, CSE and PCA are used to explore the usefulness of each feature and reduce the multi dimensional features to simplified features with no underlying hidden structure. In this paper, we take advantage of the simplified features and classifier to categorize images object with the hope to detect dangerous weapons effectively. In order to validate the effectiveness of the UEM classifier, several classifiers are used to compare the overall accuracy of the system with the compliment from the features reduction of CSE and PCA. These unsupervised classifiers include Farthest First, Density-based Clustering and k-Means methods. The final outcome of this research clearly indicates that UEM has the ability in improving the classification accuracy using the extracted features from the multi-dimensional feature reduction of CSE. Besides, it is also shown that PCA is able to speed-up the computational time with the reduced dimensionality of the features compromising the slight decrease of accuracy.

Keywords: Consistency Subset Evaluator, Principal Component Analysis, Unsupervised Expectation Maximization, Classification, Imaging surveillance

1. INTRODUCTION

Security surveillance systems are becoming indispensable in scenarios where personal safety could be jeopardized due to criminal activities [1]. Conventional security surveillance systems require the constant attention of security personnel, who monitor several locations concurrently [2,3]. Hence, the advancement in image processing techniques has become an advantage to the security surveillance systems to improve on the operational activity for monitoring purpose.

Image classification is an essential process in image processing and its major issue lies in categorizing images with huge number of input features using traditional classification algorithm. These algorithms tend to produce unstable prediction models with low generalization performance [4]. To overcome high dimensionality, image classification usually relies on a pre-processing step, specifically to extract a reduced set of meaningful features from the initial set of huge number of input features. Recent advances in classification algorithm have produced new methods that are able to handle more complex problems.

In this paper, we emphasize on the analysis and usage of the multi-dimensional features reduction on advanced classification method of Unsupervised Expectation Maximization (UEM) to classify dangerous weapons within an image. In order to validate the effectiveness of the feature reduction method and classifier, several classifiers such as Farthest First, Density-based Clustering and k-Means methods are utilized to compare the overall accuracy of the classifiers. Finally, the study depicts the comparative analysis of different classification techniques with respect to the robustness of the meaningful extracted features. The classification process comprised of four steps, which are feature extraction, training, prediction and assessing the accuracy of the classification. Analysis on the features is done to ensure the robustness and usefulness of each feature to differentiate classes effectively. The details of the classification will be discussed in this paper.

This paper is divided into four sections. Section II presents the methodology and the dataset used in this paper. In this section, the basic concept of Consistency Subset Evaluator (CSE), Principal Component Analysis (PCA), Expectation Maximization (UEM), Farthest First, Density-based Clustering and k-Means methods are discussed. Section III describes the results and discussion for the findings of the classification process using the aforementioned classifiers. The accuracy assessment with the comparisons between the classifiers is discussed in this section. In Section IV, we conclude this paper with the suggestion on future work.

2. METHODOLOGY

2.1 Data Description

In this paper, we utilized on a set of data which was available freely in the internet [5] to carry out some experimental research on the classification. We evaluated the selected algorithms using the training dataset which contains 13 features (attributes value of the image objects) with their associate class labels (Human, Bull, Child, Dog, Duck, Knife classes). Besides, 6 test dataset that contain the same features value of the image objects for each class have been identified. Feature extraction process was carried out to extract all useful features from 128 binary images (black and white images) to represent the characteristics of the image object. From the image analysis and feature extraction, 13 important and useful features of the image object as the attributes of the dataset were obtained. In this case, the extracted features must be robust enough and RST (rotation, scale and transition) invariant. A very adaptive feature would be RST-invariant, meaning that if the image object is rotated, shrunk or enlarge or translated, the value of the feature will not

change. We took the invariance of each feature into consideration and the features comprised of compactness, elongation, ratio of major axis length and minor axis length, hull ratio, moment, area ellipse ratio, axis ratio, ratio between area of the bounding box minus area of the blob and area of the bounding box, ratio between the height and the width of the bounding box, ratio between the squared perimeter and the area of the blob, roughness, ratio of the area of the blob and the area of the bounding box and compactness circularity of the blob.

2.2 Multi-dimensional Feature Reduction Methods

Feature reduction process can be viewed as a preprocessing step which removes distracting variance from a dataset, so that classifiers can perform better. In this paper, we present two multi-dimensional feature reduction methods, namely Consistency Subset Evaluator (CSE) and Principal Component Analysis (PCA).

2.2.1 Consistency Subset Evaluator (CSE)

Class consistency has been used as an evaluation metric by several approaches to attribute subset evaluation [6-8]. Attribute subset evaluation is done to look for combinations of attributes whose values divide the data into subsets containing a strong single class majority [9]. The search is in favor of small feature subsets with high class consistency. This consistency subset evaluator uses the consistency metric presented by H. Liu et al. as shown in Equation (1)

$$Consistency_s = 1 - \frac{\sum_{i=0}^J |D_i| - |M_i|}{N} \quad (1)$$

where s is an attribute subset, J is the number of distinct combinations of attribute values for s , $|D_i|$ is the number of occurrences of the i th attribute value combination, $|M_i|$ is the cardinality of the majority class for the i th attribute value combination and N is the total number of instances in the data set [9].

To use the Consistency Subset Evaluator, the dataset needs to be discretized with numeric attributes using any suitable method such as the method of U. M. Fayyad et al. [10]. The search method that can be used is the forward selection search which is to produce a list of attributes [11]. The attributes are then ranked according to their overall contribution to the consistency of the attribute set.

2.2.2 Principal Component Analysis (PCA)

Principal component analysis (PCA) is one of the most popular multi dimensional features reduction products derived from the applied linear algebra. PCA is used abundantly because it is a simple and non-parametric technique of extracting relevant information from complex data sets. The goal of PCA is to reduce the dimensionality of the data while retaining as much as possible of the variation in the original dataset.

Suppose x_1, x_2, \dots, x_N are $N \times 1$ vectors.

Step 1: Mean value is calculated with Equation (2).

$$\bar{x} = \frac{1}{N} \sum_{i=1}^N x_i \quad (2)$$

Step 2: Each features is used to subtract the mean value, shown in Equation (3).

$$\Phi_i = x_i - \bar{x} \quad (3)$$

Step 3: Matrix $A = [\Phi_1 \ \Phi_2 \ \dots \ \Phi_N]$ is generated with $N \times N$ matrix and covariance matrix with the same dimension size is computed as Equation (4) [12].

$$C = \frac{1}{M} \sum_{i=1}^N \Phi_i \Phi_i^T = AA^T \quad (4)$$

The covariance matrix characterizes the distribution of the data.

Step 4: Eigenvalues is computed:

$$C = \lambda_1 > \lambda_2 > \dots > \lambda_N \quad (5)$$

Step 5: Eigenvector is computed:

$$C = u_1, u_2, \dots, u_N \quad (6)$$

Since C is symmetric, u_1, u_2, \dots, u_N form a basis, $(x - \bar{x})$, can be written as a linear combination of the eigenvectors):

$$x - \bar{x} = b_1 u_1 + b_2 u_2 + \dots + b_N u_N = \sum_{i=1}^N b_i u_i \quad (7)$$

Step 6: For dimensionality reduction, it keeps only the terms corresponding to the K largest eigenvalues [13]

$$x - \bar{x} = \sum_{i=1}^K b_i u_i \quad \text{where } K \ll N \quad (8)$$

The representation of x into the basis u_1, u_2, \dots, u_K is thus

$$\begin{bmatrix} b_1 \\ b_2 \\ \dots \\ b_K \end{bmatrix} \quad (9)$$

2.3 Classification Methods

The aim is to do comparison of supervised classification methods for classification of the image object to their known class from the reduced multi-dimensional features dataset. The issue in identifying the most promising classification method to do pattern classification is still in research. Therefore, we are interested in predicting the most promising classification method for pattern classification in terms of the classification accuracy achieved in detecting dangerous weapons. The algorithms considered in this study are UEM, Farthest First, Density-based Clustering and k-Means. The methodology for each classifier is presented with basic concept and background.

2.3.1 Unsupervised Expectation Maximization (UEM)

The algorithm is in a model-based methods group which hypothesizes a model for each of the clusters and finds the best fit of the data to the given model [14]. Expectation Maximization performs the unsupervised classification or learning based on statistical modeling [15].

A cluster can be represented mathematically by a parametric probability distribution

$$P(x_i \in C_k) = p(C_k | x_i) = \frac{p(C_k) p(x_i | C_k)}{p(x_i)} \quad (10)$$

where each object x_i is assigned to cluster C_k and $p(x_i | C_k) = N(m_k, E_k(x_i))$ follows the normal distribution around mean, m_k , with expectation, E_k [16]. The entire data is a mixture of these distributions where each individual distribution is typically referred to as a component distribution which makes use of the finite Gaussian mixture models. So, clustering the data can be done by using a finite mixture density model of k probability distribution [17].

This algorithm can be used to find the parameter estimates for the probability distribution. It assigns each object to a cluster according to a weight representing the probability of membership [16]. Basically the algorithm consists of two main steps which are the Expectation step and the Maximization step. The Expectation step calculates the probability of cluster membership of

object x_i , for each cluster and these probabilities are the expected cluster membership for object x_i . On the other hand, the Maximization step uses the probability estimates to re-estimate the model parameters. The Expectation step can be interpreted as constructing a local lower-bound to the posterior distribution, whereas the Maximization step optimizes the bound, thereby improving the estimate for the unknowns [18]. The parameters found on the Maximization step are then used to begin another Expectation step, and the process is repeated [19].

2.3.2 Farthest First Classifier

Farthest First is a unique clustering algorithm that combines hierarchical clustering and distance based clustering. It uses the basic idea of agglomerative hierarchical clustering in combination with a distance measurement criterion that is similar to the one used by K-Means. Farthest-First assigns a center to a random point, and then computes the k most distant points [20].

This algorithm works by first select an instance to be a cluster centroid randomly and it will then compute the distance between each remaining instance and its nearest centroid. The algorithm decides that the farthest instance away from its closed centroid as a cluster centroid. The process is repeated until the number of clusters is greater than a predetermined threshold value [21].

2.3.3 Density-based Clustering Classifier

Density based algorithms typically regard clusters as dense regions of objects in the data space that are separated by regions of low density [22]. The main idea of density-based approach is to find regions of low and high density. A common way is to divide the high dimensional feature space into density-based grid units. Units containing relatively high densities are the cluster centers and the boundaries between clusters fall in the regions of low-density units [23].

This method of clustering also known as a set of density-connected objects that is maximal with respect to density-reachability [22]. Regions with a high density of points depict the existence of clusters while regions with a low density of points indicate clusters of noise or clusters of outliers. For each point of a cluster, the neighbourhood of a given radius has to contain at least a minimum number of points, which is, the density in the neighbourhood has to exceed some predefined threshold. This algorithm needs three input parameters, which comprised of the neighbour list size, the radius that delimitate the neighbourhood area of a point, and the minimum number of points that must exist in the radius that delimitate the neighborhood area of a point [24].

2.3.4 K-Means Classifier

K-Means is one of the simplest unsupervised learning algorithms that solve clustering problem. K-Means algorithm takes the input parameter and partitions a set of n objects into k clusters so that the resulting intracluster similarity is high but the intercluster similarity is low [25]. Cluster similarity is measured in regard to the mean value of the object in a cluster which can be viewed as the centroid of the cluster.

The k-Means algorithm randomly selects k of the objects, each of which initially represents a cluster mean or center. For each of the remaining objects, an object is assigned to the cluster to which it is the most similar based on the distance between the object and cluster mean. Then, it computes the new mean for each cluster and this process iterates until the criterion function converges [26]. The algorithm works well when the clusters are compact clouds that are rather well separate from one another. The method is relatively scalable and efficient in processing large data sets because the computational complexity of the algorithm [27-28].

3. RESULTS AND DISCUSSION

In this study, before any classification is applied on the dataset, CSE and PCA are used to explore the usefulness of each feature and reduce the multi dimensional features to simplified features with no underlying hidden structure. The distributions of each feature are drawn and analyzed statistically. Figure 1 shows the distributions for the features which are discarded after CSE implementation. These features include ratio of major axis length and minor axis length, ratio between the squared perimeter and the area of the blob and ratio of the area of the blob and the area of the bounding box. On the other hand, Figure 2 shows the distributions for the features which are discarded after PCA implementation and these features comprised of hull ratio, axis ratio, ratio between area of the bounding box minus area of the blob and area of the bounding box, ratio of the area of the blob and the area of the bounding box and compactness circularity of the blob

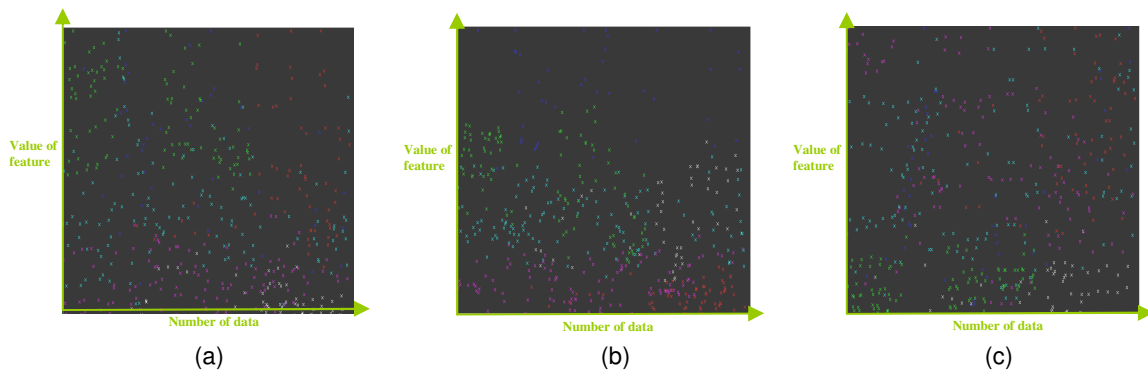


FIGURE 1: The distributions of features which are being discarded after CSE implementation (a) ratio of major axis length and minor axis length, (b) ratio between the squared perimeter and the area of the blob and (c) ratio of the area of the blob and the area of the bounding box

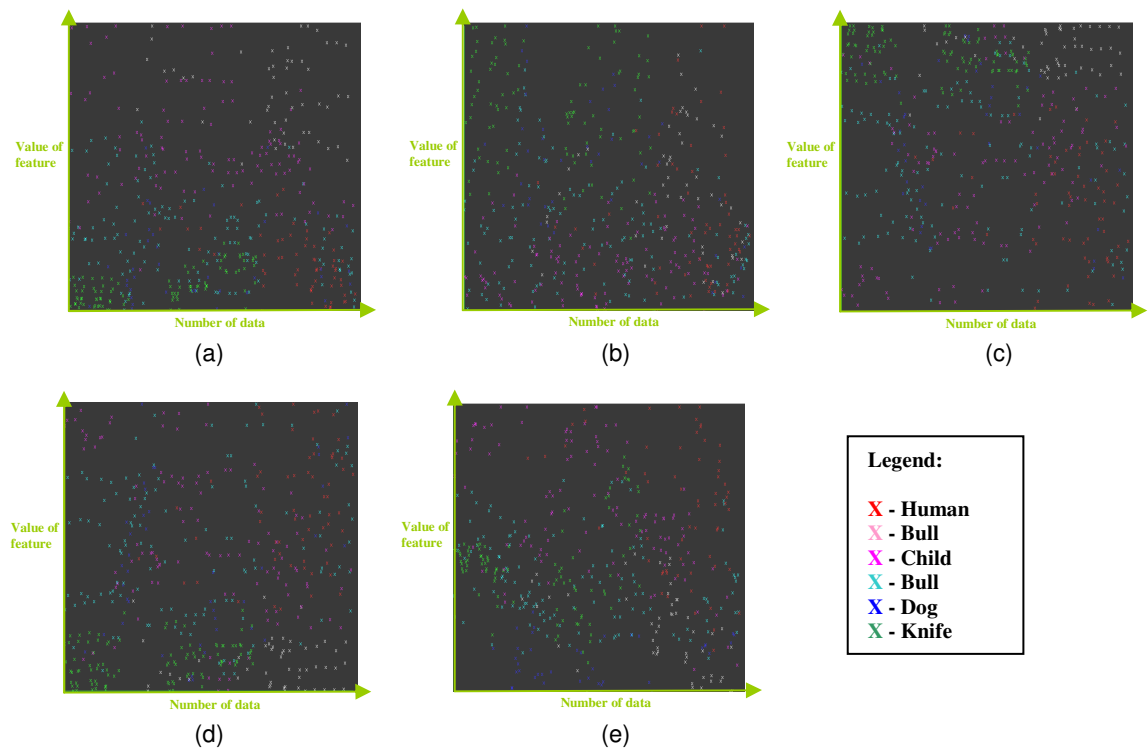


FIGURE 2: The distributions of features which are being discarded after PCA implementation (a) hull ratio, (b) axis ratio, (c) ratio between area of the bounding box minus area of the blob and area of the bounding

box, (d) ratio of the area of the blob and the area of the bounding box and (e) compactness circularity of the blob

The unsupervised classification algorithms, including UEM, Farthest First, Density-based Clustering, and k-Means classifiers are applied to the datasets. In order to validate the impact of multi dimensional feature reduction methods of CSE and PCA, four types of dataset are utilized , namely the original data, data produced after CSE method, data produced after PCA method and data produced after CSE and PCA methods. The classifiers are analyzed and the accuracy assessment is as shown in Table 1 with the computational speed (shown in bracket). In this study, the model with the highest classification accuracy is considered as the best model for pattern classification of this dataset.

	Original data (13 features)	CSE + Classifier	PCA + Classifier	CSE + PCA + Classifier
Expectation Maximization	93.33 % (8.12ms)	95 .83% (7.18ms)	90.12 % (6.21)	92.29 % (4.88ms)
Farthest First	81.88 % (7.33ms)	83.54 % (6.09ms)	82.08 % (5.65ms)	86.25 % (4.26ms)
Density based Clusterer	85.21 % (8.35ms)	88.33% (7.27ms)	87.71 % (6.51ms)	80.21% (4.93ms)
K-Means	86.04 % (7.45ms)	86.88 % (6.15ms)	89.38 % (5.69ms)	81.67% (4.37ms)

Table 1 : Accuracy Assessment and Computational Speed of Experimental Methods on Different Datasets

Based on Table 1, we can see that CSE + UEM classifier achieve the highest overall classification accuracy of all the different datasets. As the dataset we used in this study is quite small and based on our research, UEM classifier is best applied to small dataset. On the other hand, the classifiers with features generated from PCA provide slightly less accuracy and computational speed compared to the classifiers using the predefined number of features. This is due to the reduced dimensional features offered by PCA which allow only the useful key features to participate in the classification process.

4. CONCLUSION

The project is aimed to investigate the performance and impact of CSE and PCA on classification in the aspect of accuracy and computational speed. The potential of each classifier has been demonstrated and the hybrid method of CSE and UEM has shown a desirable result in detecting weapons compared to other classifiers. Our future work shall extend this work to multiple type of images and real-time signal data.

5. REFERENCES

1. A.T. Ali, and E.L. Dagless. "Computer vision for security surveillance and movement control", IEE Colloquium on Electronic Images and Image Processing in Security and Forensic Science, pp. 1-7, 1990.
2. A.C.M. Fong. "Web-based intelligent surveillance systems for detection of criminal activities", Journal of Computing and Control Engineering, 12(6), pp. 263-270, 2001.

3. Y. T. Chien, Y. S. Huang, S. W. Jeng, Y. H. Tasi, and H. X. Zhao. "A real-time security surveillance system for personal authentication". IEEE 37th Annual 2003 International Carnahan Conference on Security Technology 2003, pp. 190-195, 2003.
4. P. Geurts. "Contribution to decision tree induction: bias/ variance tradeoff and time series classification". PhD. Thesis, Department of Electrical Engineering and Computer Science, University of Liege, May 2002.
5. <http://www.cs.sdce.edu/ShapeMatcher/>.
6. H. Almuallim and T. G. Dietterich. "Learning with many irrelevant features". Proceedings of the Ninth National Conference on Artificial Intelligence, pp. 547-552, 1991.
7. H. Liu and R. Setiono. "A probabilistic approach to feature selection". Proceedings of the 13th International Conference on Machine Learning. pp. 319-327, 1996.
8. M. A. Hall and G. Holmes. "Benchmarking Attribute Selection Techniques for Discrete Class Data Mining". IEEE Transactions On Knowledge And Data Engineering, 15(3), 2003.
9. I. Kononenko. "Estimating attributes: Analysis and extensions of relief". Proceedings of the Seventh European Conference on Machine Learning, pp. 171-182, 1994.
10. U. M. Fayyad and K. B. Irani. "Multi-interval discretisation of continuous-valued attributes". Proceedings of the Thirteenth International Joint Conference on Artificial Intelligence, pp. 1022-1027, 1993.
11. M. A. Aizerman, E. M. Braverman, and L.I. Rozoner. "Theoretical foundations of the potential function method in pattern recognition learning". Automation and Remote Control, 25:826-837, 1964.
12. M. E. Tipping and C. M. Bishop. "Mixtures of probabilistic principal component analyzers". Neural Computation, 11(2): 443-482, 1999.
13. M. E. Tipping and C. M. Bishop. "Probabilistic principal component analysis". Journal of the Royal Statistical Society, 61(3): 611, 1999.
14. A. Basilevsky. "Statistical Factor Analysis and Related Methods". Wiley, New York, 1994.
15. J. Han and M. Kamber. "Data Mining: Concepts and Techniques". Morgan Kaufmann, San Francisco, CA (2001).
16. I. Borg and P. Groenen. "Modern Multidimensional Scaling: Theory and Applications". Springer (1997).
17. T. F. Cox and M. A. A. Cox. "Multidimensional Scaling". Chapman and Hall (2001).
18. S. T. Roweis and L. K. Saul. "Nonlinear dimensionality reduction by locally linear embedding". Science, 290(2):2323-2326, 2000.
19. F. Dellaert. "The Expectation Maximization Algorithm, College of Computing, Georgia Institute of Technology". Technical Report, 2002.
20. S. D. Hochbaum and B. D. Shmoys. "A Best Possible Heuristic for the k-Center Problem". Mathematics of Operational Research, 10(2): pp. 180-184, 1985.
21. S. Dasgupta and P. M. Long. "Performance guarantees for hierarchical clustering". Journal of Computer and System Sciences, 70(4):555-569, 2005.
22. X. Zheng, Z. Cai and Q. Li. "An experimental comparison of three kinds of clustering algorithms". IEEE International Conference on Neural Networks and Brain, pp. 767 -771, 2005.
23. M. Rehman and S. A. Mehdi. "Comparison of density-based clustering algorithms". Lahore College for Women University, Lahore, Pakistan, University of Management and Technology, Lahore, Pakistan.
24. M. Ester, H. P. Kriegel, J. Sander and X. Xu, "A density-based algorithm for discovering clusters in large spatial databases with noise". The 2nd International Conference on Knowledge Discovery and Data Mining, Portland, Oregon, USA, 1996.
25. K. Alsabti, S. Ranka and V. Singh. "An efficient k-Means clustering algorithm". Available online at <http://www.cise.ufl.edu/~ranka/1997>.
26. T. H. Cormen, C. E. Leiserson and R. L. Rivest. "Introduction to algorithms". McGraw-Hill Book Company, 1990.
27. R. C. Dubes and A. K. Jain. "Algorithms for clustering data". Prentice Hall (1998).

28. T. Zhang, R. Ramakrishnan and M. Livny. "An efficient Data Clustering Method for very large databases". Proceedings of the 1996 ACM Sigmod International Conference on Management of Data, Montreal, Canada, pp.103-114, 1996.

Segmentation of Brain MR Images for Tumor Extraction by Combining Kmeans Clustering and Perona-Malik Anisotropic Diffusion Model

M. Masroor Ahmed

*Faculty of Computer Science & Information System
University Teknologi Malaysia
Johor Bahru, 81310, Malaysia*

masroorahmed@gmail.com

Dzulkifli Bin Mohamad

*Faculty of Computer Science & Information System
University Teknologi Malaysia
Johor Bahru, 81310, Malaysia*

dzulkifli@utm.my

Abstract

Segmentation of images holds an important position in the area of image processing. It becomes more important while typically dealing with medical images where pre-surgery and post surgery decisions are required for the purpose of initiating and speeding up the recovery process [5] Computer aided detection of abnormal growth of tissues is primarily motivated by the necessity of achieving maximum possible accuracy. Manual segmentation of these abnormal tissues cannot be compared with modern day's high speed computing machines which enable us to visually observe the volume and location of unwanted tissues. A well known segmentation problem within MRI is the task of labeling voxels according to their tissue type which include White Matter (WM), Grey Matter (GM) , Cerebrospinal Fluid (CSF) and sometimes pathological tissues like tumor etc. This paper describes an efficient method for automatic brain tumor segmentation for the extraction of tumor tissues from MR images. It combines Perona and Malik anisotropic diffusion model for image enhancement and Kmeans clustering technique for grouping tissues belonging to a specific group. The proposed method uses T1, T2 and PD weighted gray level intensity images. The proposed technique produced appreciative results

Keywords: White Matter (WM), Gray Matter (GM), Cerebrospinal Fluid (CSF)

1. INTRODUCTION

The developments in the application of information technology have completely changed the world. The obvious reason for the introduction of computer systems is: reliability, accuracy, simplicity and ease of use. Besides, the customization and optimization features of a computer system stand among the major driving forces in adopting and subsequently strengthening the computer aided systems. In medical imaging, an image is captured, digitized and processed for doing segmentation and for extracting important information. Manual segmentation is an alternate method for segmenting an image. This method is not only tedious and time consuming, but also

produces inaccurate results. Segmentation by experts is variable [16]. Therefore, there is a strong need to have some efficient computer based system that accurately defines the boundaries of brain tissues along with minimizing the chances of user interaction with the system [3]. Additionally, manual segmentation process require at least three hours to complete [1] According to [2] the traditional methods for measuring tumor volumes are not reliable and are error sensitive.

2. PREVIOUS WORK

Various segmentation methods have been cited in the literature for improving the segmentation processes and for introducing maximum possible reliability, for example:

2.1 Segmentation by Thresholding

Thresholding method is frequently used for image segmentation. This is simple and effective segmentation method for images with different intensities. [6] The technique basically attempts for finding a threshold value, which enables the classification of pixels into different categories. A major weakness of this segmentation mode is that: it generates only two classes. Therefore, this method fails to deal with multichannel images. Beside, it also ignores the spatial characteristics due to which an image becomes noise sensitive and undergoes intensity in-homogeneity problem, which are expected to be found in MRI. Both these features create the possibility for corrupting the histogram of the image. For overcoming these problems various versions of thresholding technique have been introduced that segments medical images by using the information based on local intensities and connectivity [7]. Though this is a simple technique, still there are some factors that can complicate the thresholding operation, for example, non-stationary and correlated noise, ambient illumination, busyness of gray levels within the object and its background, inadequate contrast, and object size not commensurate with the scene. [8]. [9] introduced a new image thresholding method based on the divergence function. In this method, the objective function is constructed using the divergence function between the classes, the object and the background. The required threshold is found where this divergence function shows a global minimum.

2.2 Region Growing Method

According to [10] Due to high reliability and accurate measurement of the dimensions and location of tumor, MRI is frequently used for observing brain pathologies. Previously, region growing and shape based methods were heavily relied upon for observing the brain pathologies. [11] Proposed a Bayes-based region growing algorithm that estimates parameters by studying characteristics in local regions and constructs the Bayes factor as a classifying criterion. The technique is not fully automatic, i.e. it requires user interaction for the selection of a seed and secondly the method fails in producing acceptable results in a natural image. It only works in homogeneous areas. Since this technique is noise sensitive, therefore, the extracted regions might have holes or even some discontinuities [7] Shape based method provides an alternative approach for the segmentation of brain tumor. But the degree of freedom for application of this method is limited too. The algorithm demands an initial contour plan for extracting the region of interest. Therefore, like region growing approach, this method is also semi automatic. Both of these methods are error sensitive because, an improper or false description of initial plan and wrong selection of the seed image will lead to disastrous results. Statistical methods and fuzzy logic approaches seems to be reliable and are the best candidates for the replacement of the above mentioned techniques.

2.3 Supervised and Un-Supervised Segmentation Methods.

Supervised and un-supervised methods for image processing are frequently applied [3] [14]. [12] Presents a technically detailed review of these techniques. [13] Attempted to segment the volume as a whole using KNN and both hard and fuzzy c-means clustering. Results showed, however, that there appears to be enough data non-uniformity between slices to prevent satisfactory

segmentation. Supervised classification enables us to have sufficient known pixels to generate representative parameters for each class of interest. In an un-supervised classification pre hand knowledge of classes is not required. It usually employs some clustering algorithm for classifying an image data. According to [14] KNN, ML and Parzen window classifiers are supervised classification algorithm. Whereas, un-supervised classification algorithm includes: K-Means, minimum distance, maximum distance and hierarchical clustering etc.

3 METHODOLOGY

A brain Image consists of four regions i.e. gray matter (GM), white matter (WM), cerebrospinal fluid (CSF) and background. These regions can be considered as four different classes. Therefore, an input image needs to be divided into these four classes. In order to avoid the chances of misclassification, the outer elliptical shaped object should be removed. By removing this object we will get rid of non brain tissues and will be left with only soft tissues. In this experiment we have used T1, T2 and PD weighted brain MRIs. These images possess same size and same pixel intensity values. The pixels from the image under consideration is supposed to be grouped in any one of the aforementioned class. Finally, by applying certain post processing operations, the tumorous region can be extracted. Figure 1 shows the methodology of this work. The process uses Kmeans algorithm for solving clustering problem this algorithm aims at minimizing an *objective function*, in this case a squared error function. Mathematically, this objective function can be represented as:

$$J = \sum_{j=1}^k \sum_{i=1}^x P x_i^{(j)} - c_j P^2$$

where $P x_i^{(j)} - c_j P^2$ is a chosen distance measure between a data point $x_i^{(j)}$ and the cluster centre c_j , is an indicator of the distance of the n data points from their respective cluster centres. Image is read from database. The image contains the skull tissues. These tissues are non brain elements. Therefore, they should be removed in the preprocessing step. The presence of these tissues might lead to misclassification.

Figure 2 shows an image of the brain with skull seen as an outer elliptical ring. In figure 3 this elliptical ring is removed and we are left with only soft tissues. This is done by employing the following morphological function, i.e. erosion and dilation. Mathematically, these functions can be expressed as:

$$A \ominus B = \{ w : B_w \subseteq A \}$$

$$A \oplus B = \bigcup_{x \in B} A_x$$

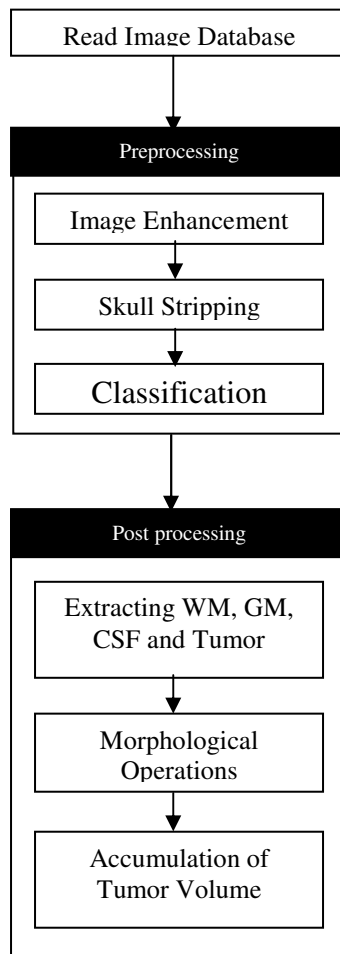
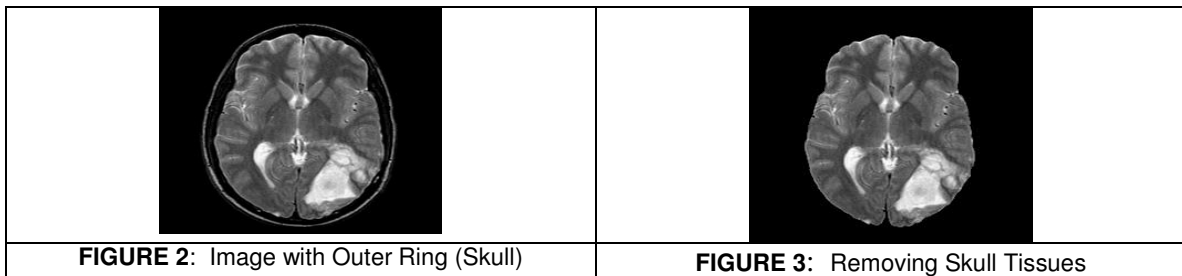


FIGURE 1: Methodology.



To test the algorithm, white gaussian noise is added to the input image. This image is then processed for enhancement. Perona and Malik [17] model is used for this purpose. This model uses partial differential equation for image denoising and enhancement. The model smooths the image without losing important details with the help of following mathematical relation [15].

$$It = \nabla \cdot [f(x, y, t) \nabla I] = \text{div}(f(x, y, t) \nabla I)$$

$I(x, y, t)$ is the intensity value of a pixel at sampling position (x, y) and scale t and $f(x, y, t)$ is the diffusivity acting on the system. The diffusivity function in Perona and Malik mode is given by the following mathematical relation

$$f(x, y, t) = f(P \nabla P^2) = \frac{1}{1 + P \nabla P^2 / k^2}$$

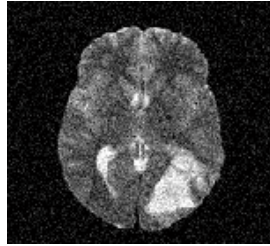


FIGURE 4: Noisy Image

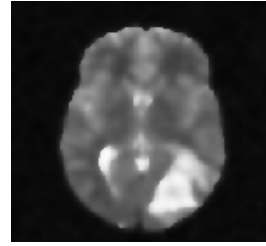
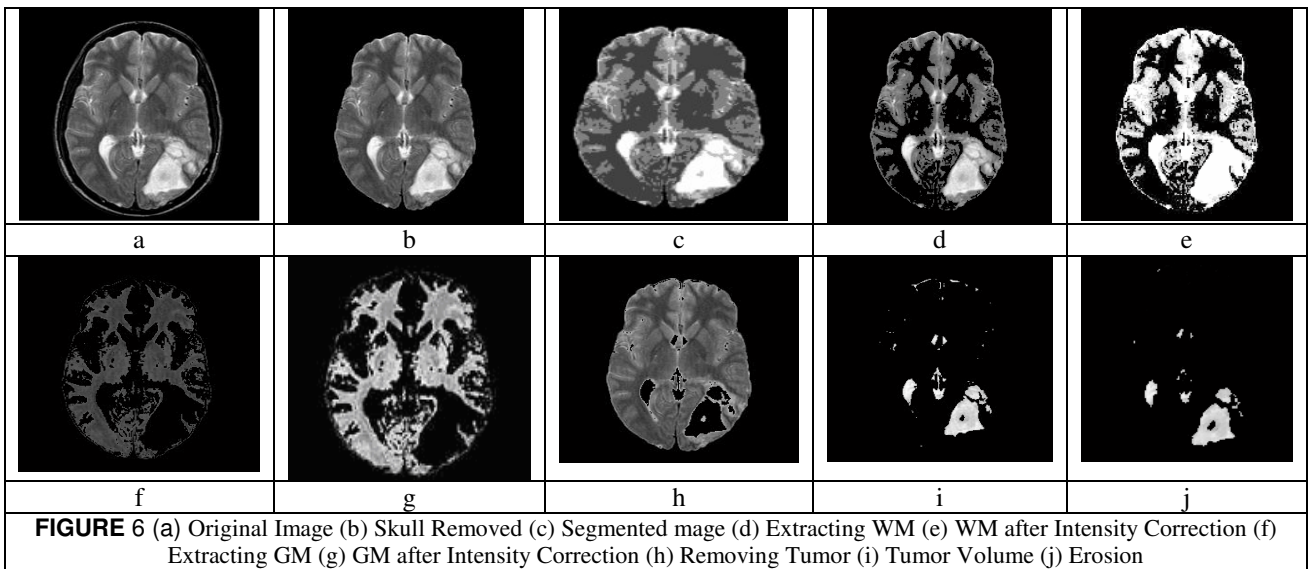


FIGURE 5: Enhanced Image

4 RESULTS AND CONCLUSION

It has been observed that when Perona and Malik model is combined with Kmeans algorithm, it produces reliable results. Due to un-supervised nature of the approach, the proposed system is efficient and is less error sensitive.



It can be deduced from the results that un-supervised segmentation methods are better than the supervised segmentation methods. Because for using supervised segmentation method a lot of pre-processing is needed. More importantly, the supervised segmentation method requires considerable amount of training and testing data which comparatively complicates the process. Whereas, this study can be applied to the minimal amount of data with reliable results. However, it may be noted that, the use of K-Means clustering method is fairly simple when compared with

frequently used fuzzy clustering methods. Efficiency and providing simple output are fundamental features of K-Means clustering method [18]. To check the accuracy of the proposed method, mean and standard deviations of clean image, noisy image containing white gaussian noise and enhanced image is drawn in Figure 7.

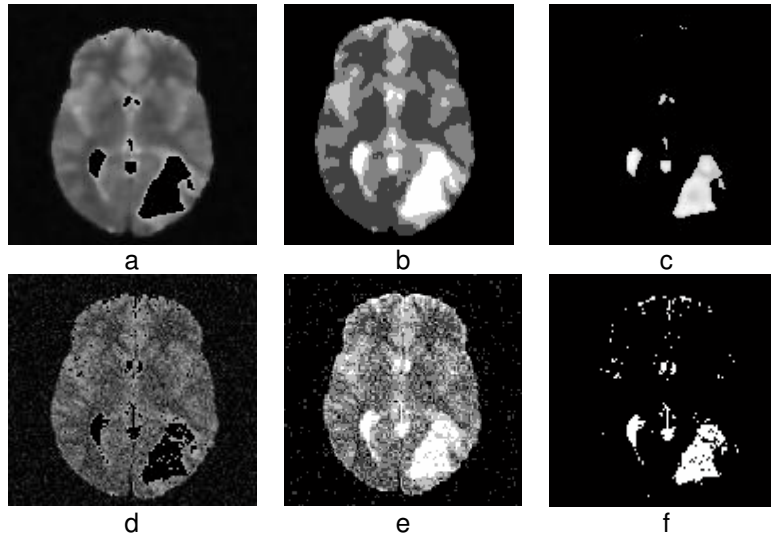


Figure 7: (a) Deleting normal tissues from enhanced MRI slice (b) Segmentation of enhanced MRI slice (c) Extraction of tumor (d) Noisy image showing only normal tissues (e) Segmentation of noisy image (f) Deleting normal tissues and retaining tumor cells.

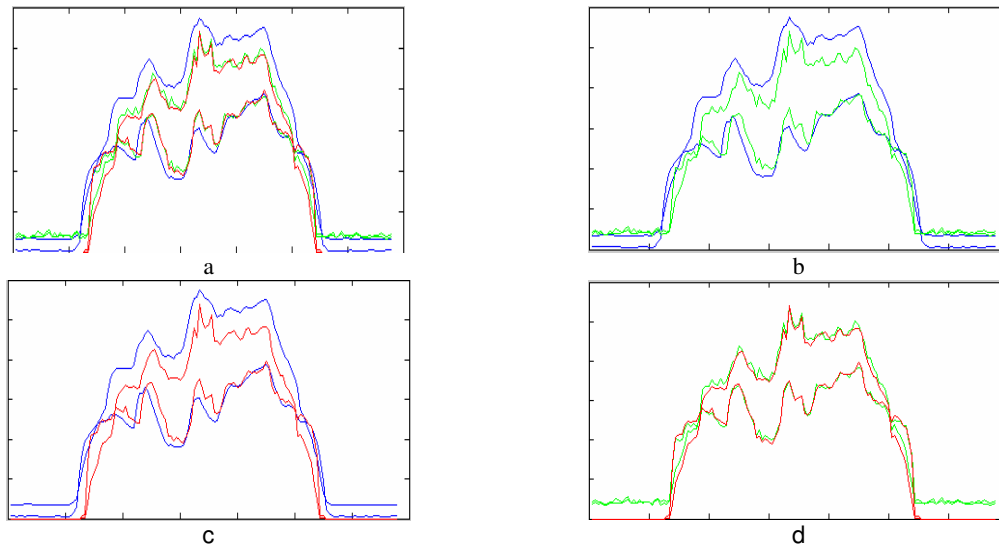


Figure 8: (a) Mean and Standard Deviations of Clean, Noisy and Enhanced Image (b) Mean and Standard Deviations of Noisy and Enhanced Image (c) Mean and Standard Deviations of clean and Enhanced Image (d) Mean and Standard Deviations of clean and Noisy Image

Figure 7 shows some results from an image enhanced by Perona-Malik anisotropic diffusion model and results from an image corrupted with with gaussian noise. There is a significant difference in both the results. Tumor extracted from a noisy image marks various portions of the MR slice which even contain the normal tissues. The results obtained from enhanced image and the clean image are almost similar. The accuracy of

the proposed method can be deduced from Figure 8 in which mean and standard deviations of MR image in various combinations is shown. Due to very less amount of noise, mean and standard deviations plotted in Figure 8 (d) shows almost the same range.

5. ACKNOWLEDGEMENTS

We would like to extend our thanks to “*Whole Brain Atlas*” for MR images.

6. REFERENCES

- [1] M. Mancas, B. Gosselin, B. Macq, 2005, "*Segmentation Using a Region Growing Thresholding*", Proc. of the Electronic Imaging Conference of the International Society for Optical Imaging (SPIE/EI 2005), San Jose (California, USA).
- [2] Dong-yong Dai; Condon, B.; Hadley, D.; Rampling, R.; Teasdale, G.; "*Intracranial deformation caused by brain tumors: assessment of 3-D surface by magnetic resonance imaging*" IEEE Transactions on Medical Imaging Volume 12, Issue 4, Dec. 1993 Page(s):693 – 702
- [3] Matthew C. Clark "*Segmenting MRI Volumes of the Brain With Knowledge- Based Clustering*" MS Thesis, Department of Computer Science and Engineering, University of South Florida, 1994
- [5] <http://noodle.med.yale.edu>
- [6] <http://documents.wolfram.com/>
- [7] Dzung L. Pham, Chenyang Xu, Jerry L. Prince; "*A Survey of Current Methods in Medical Medical Image Segmentation*" Technical Report JHU / ECE 99-01, Department of Electrical and Computer Engineering. The Johns Hopkins University, Baltimore MD 21218, 1998.
- [8] M. Sezgin, B. Sankur " *Survey over image thresholding techniques and quantitative performance evaluation*" J. Electron. Imaging 13 (1) (2004) 146-165.
- [9] Chowdhury, M.H.; Little, W.D.; "*Image thresholding techniques*" IEEE Pacific Rim Conference on Communications, Computers, and Signal Processing, 1995. Proceedings. 17-19 May 1995 Page(s):585 – 589
- [10] Zhou, J.; Chan, K.L.; Chong, V.F.H.; Krishnan, S.M "*Extraction of Brain Tumor from MR Images Using One-Class Support Vector Machine*" 27th Annual International Conference of the Engineering in Medicine and Biology Society, 2005. IEEE-EMBS 2005, Page(s):6411 – 6414
- [11] Pan, Zhigeng; Lu, Jianfeng; "*A Bayes-Based Region-Growing Algorithm for Medical Image Segmentation*" Computing in Science & Engineering, Volume 9, Issue 4, July-Aug. 2007 Page(s):32 – 38
- [12] J. C. Bezdek, L. O. Hall, L. P. Clarke "Review of MR image segmentation techniques using pattern recognition. " Medical Physics vol. 20, no. 4, pp. 1033 (1993).
- [13] Velthuizen RP, Clarke LP, Phuphanich S, Hall LO, Bensaid AM, Arrington JA, Greenberg HM and Silbiger ML. "*Unsupervised Tumor Volume Measurement Using Magnetic Resonance Brain Images*," Journal of Magnetic Resonance Imaging , Vol. 5, No. 5, pp. 594-605, 1995.

- [14] Guillermo N. Abras and Virginia L. Ballarin,; "A Weighted K-means Algorithm applied to Brain Tissue Classification", JCS&T Vol. 5 No. 3, October 2005.
- [15] Izquierdo, E.; Li-Qun Xu;Image segmentation using data-modulated nonlinear diffusion Electronics Letters Volume 36, Issue 21, 12 Oct. 2000 Page(s):1767 – 1769
- [16] S. Wareld, J. Dengler, J. Zaers, C. Guttman, W. Gil, J. Ettinger, J. Hiller, and R. Kikinis. "Automatic identification of grey matter structures from mri to improve the segmentation of white matter lesions". J. of Image Guided Surgery, 1(6):326{338, 1995.
- [17] Perona, P.; Malik, J.; "Scale-space and edge detection using anisotropic diffusion" Pattern Analysis and Machine Intelligence, IEEE Transactions on Volume 12, Issue 7, July 1990 Page(s):629 – 639
- [18] Dmitriy Fradkin, Ilya Muchnik (2004)"A Study of K-Means Clustering for Improving Classification Accuracy of Multi-Class SVM". Technical Report. Rutgers University, New Brunswick, New Jersey 08854, April, 2004.



COMPUTER SCIENCE JOURNALS SDN BHD
M-3-19, PLAZA DAMAS
SRI HARTAMAS
50480, KUALA LUMPUR
MALAYSIA